Response of the BGO Calorimeter to Cosmic-Ray Nuclei in the DAMPE Experiment on Orbit

H. T. Dai, Y. L. Zhang, J. J. Zang, Z. Y. Zhang, Y. F. Wei, L. B. Wu, C. M. Liu, C. N. Luo, D. Kyratzis, A. De Benedittis, C. Zhao, Y. Wang, P. C. Jiang, Y. Z. Wang, Y. Z. Zhao, X. L. Wang, Z. Z. Xu, and G. S. Huang

***Abstract*— DArk Matter Particle Explorer (DAMPE), a satellite-based cosmic-ray (CR) and gamma-ray measurement experiment, relies on its calorimeter to measure the energy of incident particles. The calorimeter adopts crystals of bismuth germanium oxide (BGO) as scintillating material, and it is designed to aim for measurements of energy ranging from 50 GeV to 100 TeV in the case of a CR nucleus. This article concerns the response of the BGO calorimeter to nucleus-type CRs. CRs with very low energy can rarely reach the detector due to the Earth's magnetic field. A cutoff on lower energy can be observed in the energy spectrum. In this article, the cutoff is used to study the response of the calorimeter. Carbon, neon, silicon, and iron are analyzed separately in comparison with Monte Carlo simulations by Geant4.**

***Index Terms*— Bismuth germanium oxide (BGO) calorimeter, cosmic-ray (CR) nuclei, DArk Matter Particle Explorer (DAMPE), energy response, geomagnetic cutoff.**

I. Introduction

FOR space experiments such as Fermi Large-Area Telescope (LAT) [1], CALorimetric Electron Telescope (CALET) [2], and DArk Matter Particle Explorer (DAMPE) [3], the detectors need to be calibrated with well-known sources of astrophysical origin. Meanwhile, even with a complete calibration, there are still too many factors that might influence the measurement and the reconstruction of science data. It is meaningful to make sure that our knowledge about the response of our instrument is reliably reflecting the reality. In order to achieve this, the geomagnetic cutoff feature in cosmic-ray (CR) spectrum can be used as a source to investigate the performance of the calorimeter. A brief introduction is given as follows.

On the orbit of DAMPE (sun-synchronous orbit with an inclination of 97° and at an altitude of 500 km), CRs with low momentum can hardly be observed, because they are bent by the Earth's magnetic field when radiating toward the Earth. The trajectory of a charged particle in a magnetic field follows the equation:

$$R = P/z \approx 0.3 \times B \times \rho \tag{1}$$

where R is the rigidity, P is the momentum of the particle (GeV/c), z is the charge number (absolute value), B is magnetic flux density (Tesla), and ρ is the radius (m). This sets R in the unit of gigavolts, representing momentum per unit of charge. The equation tells us that CRs carrying the same charge are more easily bent with lower momentum. At different position over the Earth, the geomagnetic cutoff in the spectrum, viewed by the DAMPE spectrometer, varies largely from ∼1 to ∼12 of GV. This makes the cutoff on the energy of CR nuclei extend from several gigaelectronvolts to hundreds of gigaelectronvolts. For example, CR iron acquired near the equator has the cutoff energy over 200 GeV.

This cutoff in the energy spectrum can also be determined numerically by tracing the CR nuclei in the magnetic field, and a comparison between the measured data and the simulated ones can be performed.

Similar work on CR electron-plus-positron (CRE) has been done by Fermi-LAT [4]. The major differences from this previous work are focused on two specific points: first the cutoff in CR nuclei spectrum is higher because particles that carry more charge are more strongly shielded by the Earth's magnetic field, i.e., nuclei with higher atomic number have higher cutoff on their energy. Second in the CR's interaction with the atmosphere, heavy ions are produced rarely, which means the cutoff in the spectrum has no secondary contamination.

The cutoff value varies at different positions near the Earth. Roughly speaking, it reaches its maximum near the equator. The analysis in this article is performed using data collected within the shaded area in Fig. 1 to study the response of the bismuth germanium oxide (BGO) calorimeter in higher energy. It is where we can get a maximum cutoff and enough data in the meantime. This area is defined by the McIlwain L interval 1.00–1.14. The McIlwain L value is a parameter describing the

Manuscript received March 1, 2020; revised April 21, 2020; accepted April 28, 2020. Date of publication May 8, 2020; date of current version June 19, 2020. This work was supported in part by the National Natural Science Foundation of China under Grant 11673021 and Grant 11705197, in part by the Joint Funds of the National Natural Science Foundation of China under Grant U1738208, Grant U1738139, and Grant U1738135, and in part by the National Key Research and Development Program of China under Grant 2016YFA0400200.

H. T. Dai, Y. L. Zhang, Z. Y. Zhang, Y. F. Wei, L. B. Wu, C. M. Liu, C. Zhao, Y. Wang, P. C. Jiang, Y. Z. Wang, Y. Z. Zhao, X. L. Wang, Z. Z. Xu, and G. S. Huang are with the State Key Laboratory of Particle Detection and Electronics, Department of Modern Physics, University of Science and Technology of China, Hefei 230026, China (e-mail: ylzhang@ustc.edu.cn; hgs@ustc.edu.cn).

J. J. Zang and C. N. Luo are with the Key Laboratory of Dark Matter and Space Astronomy, Purple Mountain Observatory, Chinese Academy of Sciences, Nanjing 210033, China.

D. Kyratzis is with the Gran Sasso Science Institute (GSSI), 67100 L'Aquila, Italy, and also with the Laboratori Nazionali del Gran Sasso, INFN Istituto Nazionale di Fisica Nucleare, 67100 L'Aquila, Italy.

A. De Benedittis is with the Dipartimento di Matematica e Fisica E. De Giorgi, Universita` del Salento, 73100 Lecce, Italy, and also with the Istituto Nazionale di Fisica Nucleare (INFN)–Sezione di Lecce, 73100 Lecce, Italy.

Color versions of one or more of the figures in this article are available online at http://ieeexplore.ieee.org.

Digital Object Identifier 10.1109/TNS.2020.2992557

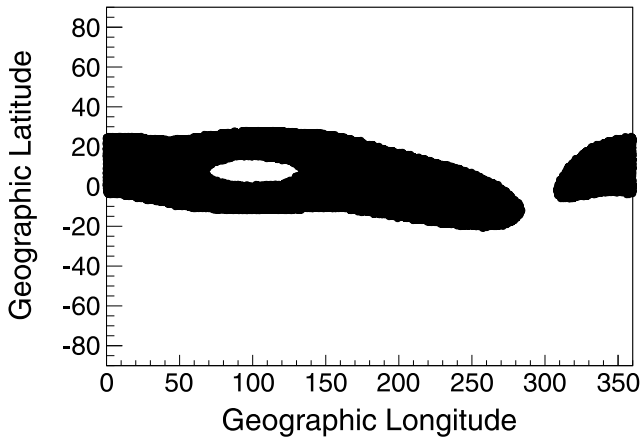

Fig. 1. Region of McIlwain L value between 1.00 and 1.14 for the orbit at an altitude of 500 km.

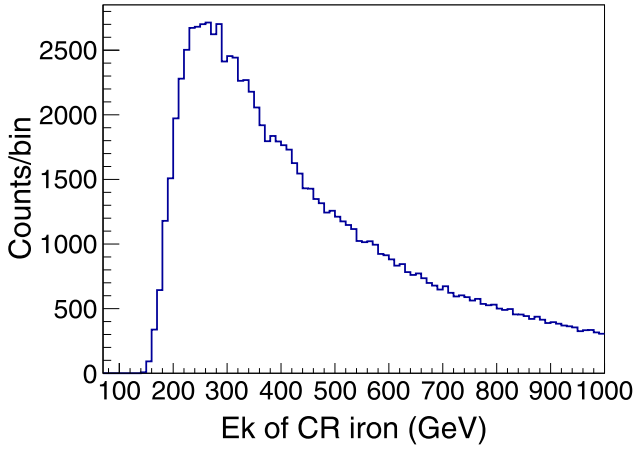

Fig. 2. Distribution of kinetic energy of CR irons that can cross the DAMPE orbit in the area of McIlwain L interval (1.00, 1.14), uniform binning adopted. It is a result of "toy" simulation, obtained simply by simulating the geomagnetic field effect on CR irons without considering any detector response. From this, we can see a clear structure of cutoff by geomagnetic effect and it is located at over 200 GeV for CR irons.

density of magnetic field lines crossing the Earth's magnetic equator, thus being an appropriate way to characterize the geomagnetic cutoff [5].

Due to the geomagnetic field, Fig. 2 represents a typical distribution of the kinetic energy of CRs. The spectrum, obtained by only simulating the geomagnetic effect, shows the energy of CR iron that can cross the DAMPE orbit within this area. The counts of CR iron rise from ∼150 GeV and reach maximum at ∼250 GeV, then slowly drop as energy goes higher. Without atmospheric contamination at low energy, the cutoff is more clearly shown and at much higher energy than the cutoff on CRE presented in [4]. Thus, it can be used as a good reference to study the response of the calorimeter to particles with higher energy. In the spectrum, the left shoulder is a rising edge instead of a cutoff at a single value, because CRs are not observed at one single position over the Earth, and they can reach the detector from different directions.

II. DAMPE Spectrometer

A. Structure of DAMPE

DAMPE is a satellite-based telescope aiming at detection of very high-energy CRs and gamma rays. Fig. 3 is a schema of it.

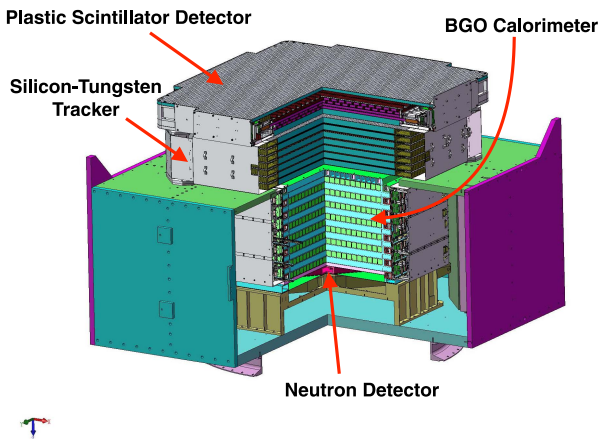

Fig. 3. Schema of DAMPE.

The whole detector consists of a plastic scintillator detector (PSD), a silicon–tungsten tracker–converter (STK), a BGO imaging calorimeter (BGO), and a neutron detector (NUD) from top to bottom [3]. The PSD is essentially utilized in order to provide the charge number (for CR nuclei, it is also the atomic number $|Z|$) of incident particles, as well as being an anticoincidence detector for γ-rays. The STK reconstructs the trajectory. The BGO calorimeter measures the energy and distinguishes electromagnetic particles from hadrons. The BGO image also gives some rough track information. The NUD provides additional electron–hadron discrimination, which is important for energy range above teraelectronvolt. The four subdetectors above provide good measurements of the charge, arrival direction, energy, and particle identification to accomplish major scientific objectives of DAMPE, including indirect search for dark matter signals, γ-ray astronomy, and studies on the origin and propagation mechanism of galactic CRs (GCRs).

B. BGO Calorimeter and Energy Measurement

The calorimeter contains 14 layers, each of 22 BGO crystal bars are arranged alternately in x- or y-direction in each layer, as shown in Fig. 4. All of the 308 BGO bars are of size 25 mm × 25 mm × 600 mm. The calorimeter is of 1.6 λ_I (nuclear interaction length) from top to bottom, which is crucial to the energy measurement of CR nuclei.

To validate the fidelity of the instrument model and the simulation, beam tests were performed in 2014 and 2015 at CERN, with high-energy gamma rays, electrons, protons, muons, and various nuclei produced by fragmentation of argon and lead on the engineering qualification model (EQM) of DAMPE [3].

The on-orbit calibration for energy measurement consists of the pedestal calibration, the zero-suppression threshold and electronics linearity, the minimum ionization particle (MIP) response calibration, the photomultiplier tube (PMT) dynode ratio calibration, and the light attenuation calibration [6]. The MIP signals by relativistic protons are compared with the distribution of deposited energies given by Monte Carlo simulations of the on-orbit spectrum of CR protons that should be detected by DAMPE. This gives the parameter of the

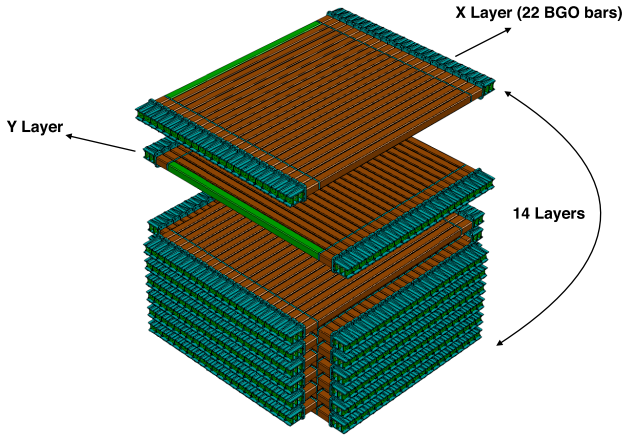

Fig. 4. Calorimeter consisting of 14 layers. Each layer has 22 BGO bars in x- or y-direction.

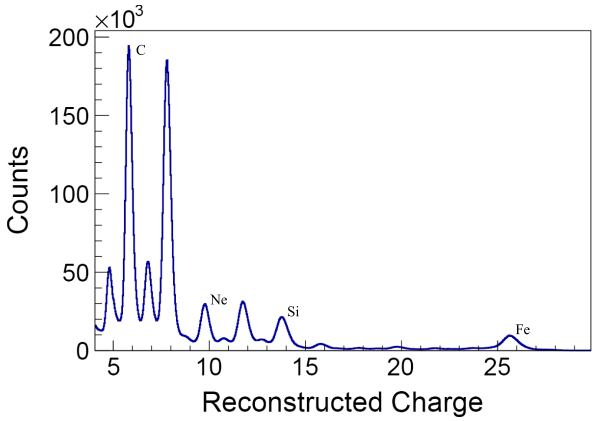

Fig. 5. Reconstructed charge by the PSD subdetector. No correction is done here so that the center value of the peaks is not forced to be an integer. Carbon, neon, silicon, and iron are picked out as four relatively abundant elements in CRs to do this analysis. Besides, they have the energy cutoff distant enough from each other.

transfer function that converts signals in digital counts to energies that a particle releases in the crystal [7].

III. Simulation of the Geomagnetic Cutoff

Particles that can reach DAMPE are subject to the primary spectrum of some certain type of CR modified by the Earth's magnetic field. When doing the simulation, the primary spectrum measured by other previous experiment is used as an input to Geant4, thus the DAMPE response simulated. The effect of the geomagnetic field is considered in the next step. The two steps are separately introduced as follows.

A. Primary Spectrum of CR Nuclei and Geant4 Simulation

As mentioned in Section I, the cutoff on energy increases as the charge number of CR nuclei gets larger. Carbon, neon, silicon, and iron are four elements chosen for investigating the BGO calorimeter response to the spectrum of geomagnetic cutoff. They are relatively abundant in CRs, and the cutoff in their energy spectrum is distinct enough from each other, so they can be used as four different sources.

The experimental result of PAMELA was adopted as the primary spectrum of CR carbon to be put into Geant4 simulation [8]. Simulation for neon used the results of HEAO-3 C2 experiment [9], silicon, and iron of ATIC02 [10]. In this step, the response of the whole DAMPE detector to the primary CR nuclei was given via Monte Carlo simulations. Then the sample was to be further simulated for a real orbit detection, using the so-called back tracing technique, within the region of McIlwain L interval 1.00–1.14. Thus, the effect of geomagnetic field would be considered.

B. Back Tracing in the Magnetic Field

The international geomagnetic reference field (IGRF) models serve as a series of standard descriptions of the Earth's magnetic field [11]. Mathematically, these models are spherically harmonic expansions of the geomagnetic potential. The version of IGRF-12 was adopted for this article. Generally, other external sources (such as solar wind) contribute little to shielding the Earth compared to the Earth's internal magnetic field [12], though the real magnetic environment around the Earth is a multisource system [13], especially when one moves farther away from the Earth. Data collected during strong geomagnetic storms [14] are excluded in the analyses, which further reduces the influence from dynamic external sources of the field.

As it is hard to trace a particle coming from the Galaxy in the Earth's magnetic field and expect it to collide with the DAMPE detector, back tracing a particle from the coordinates of DAMPE to see whether it comes from the Galaxy or not would be a more practical way. A particle can be back traced from the position where the DAMPE satellite is located, and if it turns out that it intersects the Earth or is captured by the Earth (back traced for a given time that is long enough and pointless to compute more), it is considered unphysical, as it cannot be a primary GCR anymore. The particle is considered galactic when it reaches ten Earth radii. The code developed by Smart and Shea [5] was used to compute the particle trajectory tracing. More detailed description of this method can be found in [4].

We simulated the DAMPE orbit from January 2016 to July 2017 and distributed some simulated events obtained by Geant4 on the location of every one second on this orbit, then back traced these events. Only the orbit in the region of McIlwain L interval 1.00–1.14 was considered.

IV. Performance of the Calorimeter

A. Selection of Data

To distinguish different elements in CRs, the event should at least have a reliable reconstructed charge in the PSD subdetector. Fig. 5 shows the charge spectrum of heavy ions detected by DAMPE. For each of the four peaks, the events within the full-width at half-maximum are taken as candidates for this element.

To measure the energy of CR nuclei, it is better to select events with a sufficiently developed shower profile for the analysis. For this, we use only high-energy triggered events and require the energy deposition maximum position to be in the first nine layers of the BGO calorimeter, and not located too much on the side. Besides, the events are selected only when it deposits energy in the third layer 1.5 times larger than in the first layer. This condition makes sure that the cascade process sufficiently develops in the BGO calorimeter as soon

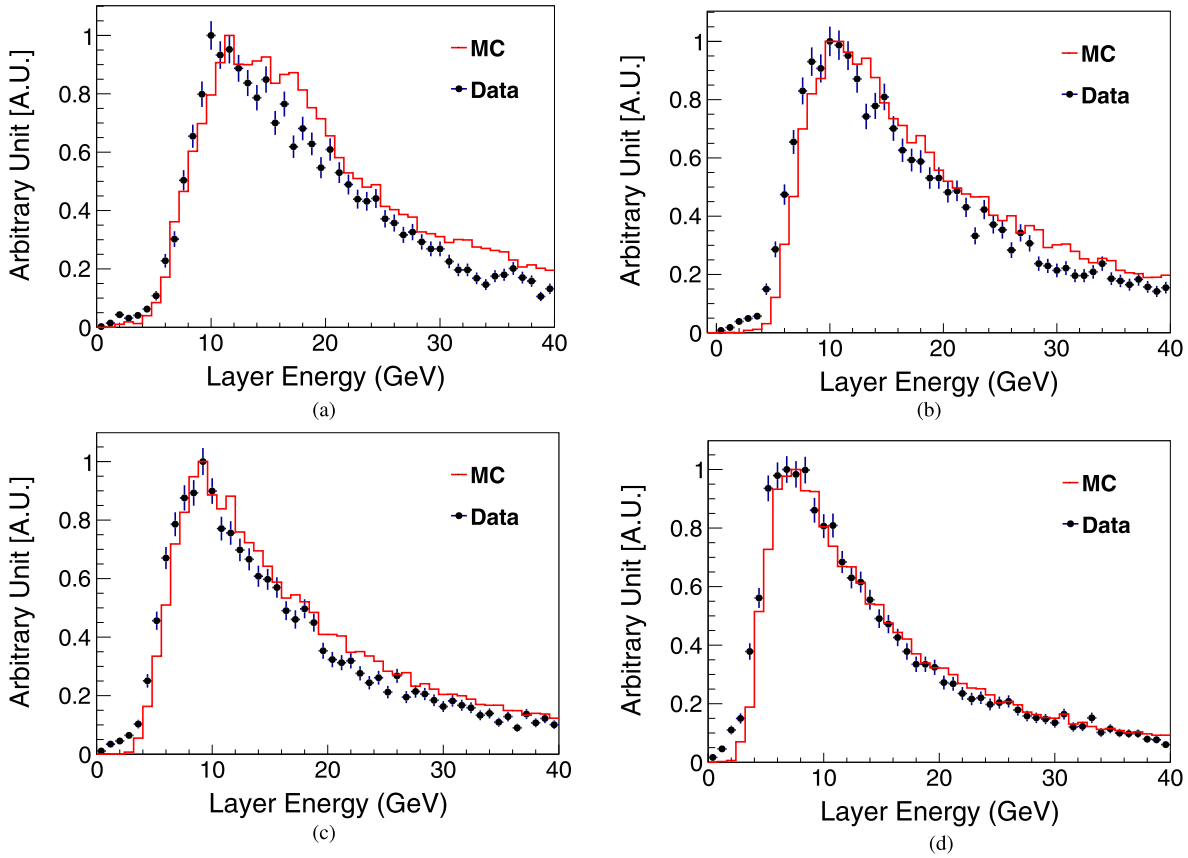

Fig. 6. Energy deposited in one layer of the BGO calorimeter. Above are four layers among the total 14 to show the comparison between data and MC, respectively, layers 2, 5, 8, and 11. Here we again take CR iron as an example. (a) Energy in layer 2. (b) Energy in layer 5. (c) Energy in layer 8. (d) Energy in layer 11.

as the particle enters. For the simulation data, all events that are classified as unphysical (that cannot be a real primary GCR) are eliminated for all the analyses in this article.

B. Validation of the Energy Deposition

It is the BGO calorimeter response to energy deposition that we want to study. Most of the effective events detected by DAMPE are coming from the top of the BGO calorimeter because of the positioning of the PSD and STK subdetectors, which provide information on the charge and track. Since the energy deposition in different layers from top to bottom reflects the longitudinal shower development, a layer-by-layer comparison between measured energy and simulation has been done. Fig. 6 is such a comparison on the energy deposition by CR irons, showing the situations within four single layers among the total 14 layers of the calorimeter. Approximately, the profile of the distribution given by simulation agrees with the measured one, but still as the particle goes deeper in the calorimeter (as the shower sufficiently develops), they agree to a better level. This might come from the uncertainty from the interaction models when the shower has not sufficiently developed, where the secondary particles of cascade are relatively less than in the deep part of the calorimeter. As for in the layer 11 (the last case in Fig. 6), the fit mean value of the distribution in flight data is 6.30 ± 0.18 GeV, while the fit mean value is 6.52 ± 0.16 GeV for simulation. Within the errors, simulation agrees well with flight data.

V. Response to CR Nuclei in the Energy Band Around the Cutoff

A. Comparison of the Total Deposited Energy

The response of the whole BGO calorimeter to CR carbon, neon, silicon, and iron can be investigated. According to the beam tests performed at CERN, the total deposited energy is estimated to be ~30%–40% of the incident energy for nuclei [3]. The deposited energy spectrum of the selected data sample has a cutoff, which locates at roughly ~30%–40% the physical energy cutoff of this CR nucleus. The spectra given by simulations and flight data are drawn together to give a visual comparison between them in Fig. 7. Generally speaking, the profile of the distribution agrees well between simulations and flight data. The measured deposited energy fluctuates around the simulation, which means the response of the BGO calorimeter agrees with our simulation models to some extent. Still, the rising edge by flight data is located a little to the left of simulations, and the agreement of the rising edge gets better as heavier CR nuclei are analyzed.

B. Fitting the Count Spectra

The count spectra of energy in Fig. 7 can be parametrized by the function below:

$$dN(E)/dE = cE^{-\gamma}/(1+e^{-a(E-E_c)}) \quad (2)$$

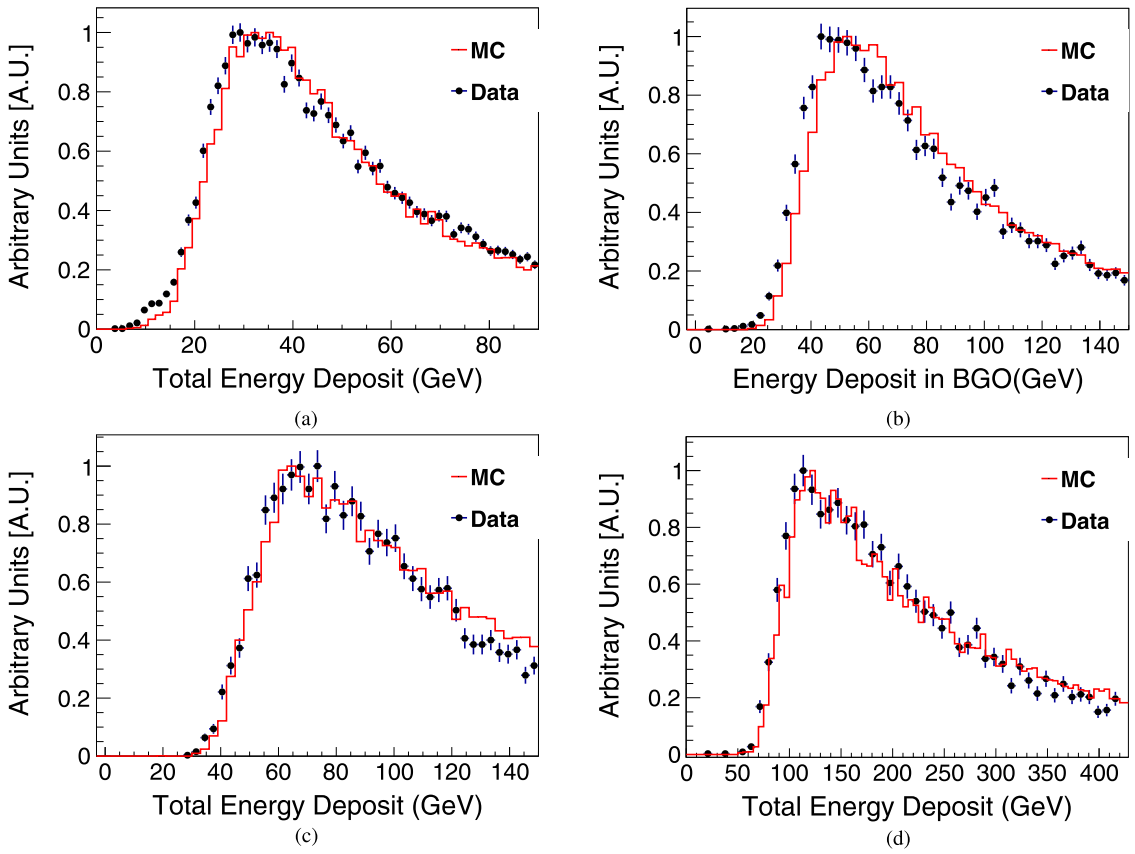

Fig. 7. Energy deposited in the BGO calorimeter, respectively, by CR carbon, neon, silicon, and iron. Flight data are set to dots, and simulations are set to red lines to show the comparison between data and MC. (a) Carbon. (b) Neon. (c) Silicon. (d) Iron.

where γ is the spectral index and E_c the cutoff energy. c stands for no special meaning but the magnitude of event counts. a is a parameter representing the steepness of the rising edge in the spectrum. The spectra of deposited energy of flight data and simulations were fit with the function separately.

Fig. 8 shows the fitting on the energy distribution of CR irons for both simulation and flight data. The same procedure was applied to the analyses of the other three elements.

C. Comparison of the Fitting Parameters

Since it is the deposited energy spectrum rather than a flux distribution on the kinetic energy, the γ parameter does not stand for the so-called "power law" index of flux studies. It was set as a free parameter and differs by ∼4% between the flight data fitting and the simulation fitting for CR irons. The parameter a differs by ∼2.5%. It is even more interesting to compare the E_c parameter. Fig. 9 gives the ratio of this parameter in the two spectra. The systematic uncertainties on this parameter are considered as follows.

For the simulation of back tracing particles in the magnetic field, the satellite experiment HEAO-3 C2 has performed a check on its rigidity cutoff measurement. The HEAO-3 C2 experiment operates during 1979–1981 on an orbit of 496 km as an altitude and 43.6° as an inclination angle. For its analysis of oxygen nuclei, they found the computed cutoffs by the back tracing method ∼3–5 ±2% higher than the measured ones. It was deduced that this systematic bias mainly came from the IGRF model [4], [15]. Directly comparing their finding with the work presented here may be difficult, although the two satellites orbit almost at the same altitude. However, the description given by the model is more reliable and accurate near the geomagnetic equator [16], which is exactly where the analyses in this article are performed, as seen in Fig. 1. Therefore, it should be safe to assume that the bias caused by the back tracing of particles would be no greater than 3%–5% estimated by the HEAO-3 C2 experiment. Their finding could serve as a conservative estimation for the bias of back tracing method while the definitive value of this bias is unknown.

The uncertainty from the Geant4 simulation is estimated according to the nuclei beam test of DAMPE. In the beam test performed in 2015 on H8 beamline at the CERN super proton synchrotron (SPS) facility, the calorimeter response to nuclei of atomic number under 18 was studied [17]. The analyses found that the deviation of Geant4 simulation from the beam test data is 1.831% for carbon, 1.721% for neon, and 0.213% for silicon at 40 GeV/n. This article does not give the specific value for iron, since the iron has atomic number higher than 18. However, it is evident that the deviation tends to be consistent with only the deviation of helium and lithium larger than the others. Only as an extrapolation, the value for iron might be roughly around 1%.

For the event selection, the uncertainty resulting from the track reconstruction is estimated as 2.5% for carbon, 3% for neon, 2% for silicon, and 3% for iron. The uncertainties from

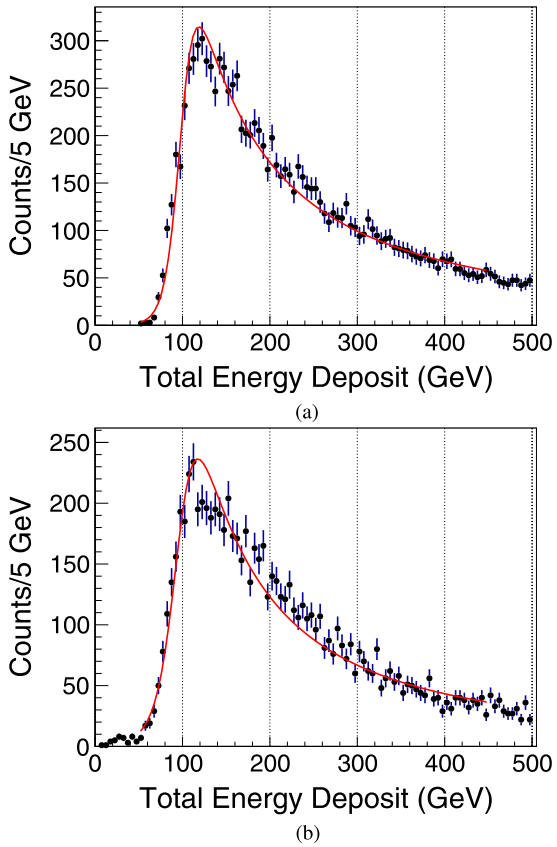

Fig. 8. Total energy deposit by CR irons in the calorimeter. The upper panel is the case for simulation, whereas the lower panel measured data. The dots represent the distribution after the selection procedure. The red line is the fit function. (a) Simulation. (b) Flight data.

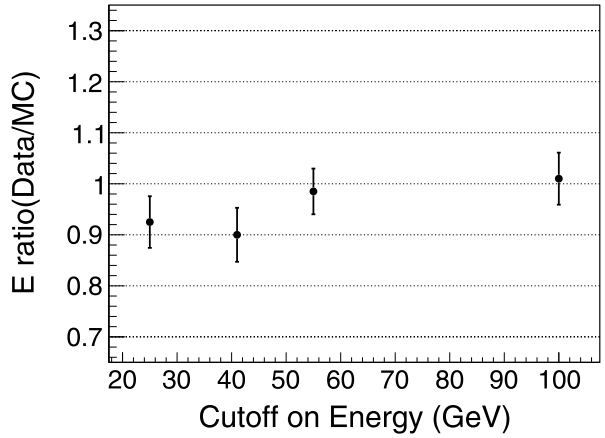

Fig. 9. Ratio between the energy cutoff on deposited energy and the energy cutoff provided by simulation. Given the uncertainties, the ratios are compatible with one.

other selections such as trigger efficiency are much less and negligible.

VI. Conclusion

The Earth's magnetic field shields the Earth from CRs of low energy. This fact leads to the geomagnetic cutoff in the energy spectrum of CRs, which can be used as a source to test the response of the BGO calorimeter. By choosing CR carbon, neon, silicon, and iron in the data of DAMPE experiment from January 2016 to July 2017, we investigated the response of the BGO calorimeter. Through a data selection, the layer energy and total energy deposits are compared between flight data and simulations. From different perspectives, the energy deposition in the BGO calorimeter exhibits a consistency between simulations and flight data. For the evaluation of the cutoff in the deposited energy spectrum, given the uncertainties, flight data generally are compatible with simulations. Especially for Fe, the two differ only by 1%, while for C and Ne, the difference is larger. All the discrepancies of the four elements in analysis are less than 10%.

References

[1] W. B. Atwood *et al.*, "The large area telescope on the Fermi gamma-ray space telescope mission," *Astrophys. J.*, vol. 697, no. 2, pp. 1071–1102, Jun. 2009.

[2] O. Adriani *et al.*, "The CALorimetric Electron Telescope (CALET) for high-energy astroparticle physics on the International Space Station," in *Proc. 24th Eur. Cosmic Ray Symp. (ECRS)* in Journal of Physics Conference Series, vol. 632. Kiel, Germany: Christian Albrechts Univ. Kiel, Sep. 2014.

[3] J. Chang *et al.*, "The DArk matter particle explorer mission," *Astropart. Phys.*, vol. 95, pp. 6–24, Oct. 2017.

[4] M. Ackermann *et al.*, "In-flight measurement of the absolute energy scale of the Fermi large area telescope," *Astropart. Phys.*, vol. 35, no. 6, pp. 346–353, 2012. [Online]. Available: http://www.sciencedirect.com/science/article/pii/S0927650511001940

[5] D. F. Smart and M. A. Shea, "A review of geomagnetic cutoff rigidities for earth-orbiting spacecraft," *Adv. Space Res.*, vol. 36, no. 10, pp. 2012–2020, Jan. 2005. [Online]. Available: http://www.sciencedirect.com/science/article/pii/S0273117705001997

[6] G. Ambrosi *et al.*, "The on-orbit calibration of DArk matter particle explorer," *Astropart. Phys.*, vol. 106, pp. 18–34, Mar. 2019.

[7] L. Wu *et al.*, "Calibration and status of the 3-D imaging calorimeter of DAMPE for cosmic ray physics on orbit," *IEEE Trans. Nucl. Sci.*, vol. 65, no. 8, pp. 2007–2012, Aug. 2018.

[8] O. Adriani *et al.*, "Measurement of boron and carbon fluxes in cosmic rays with the PAMELA experiment," *Astrophys. J.*, vol. 791, no. 2, p. 93, Jul. 2014, doi: 10.1088%2F0004-637x%2F791%2F2%2F93.

[9] J. J. Engelmann *et al.*, "Charge composition and energy spectra of cosmic-ray nuclei for elements from Be to Ni—Results from HEAO-3-C2," *Astron. Astrophys.*, vol. 233, no. 1, pp. 96–111, Jul. 1990.

[10] A. D. Panov *et al.*, "Energy spectra of abundant nuclei of primary cosmic rays from the data of ATIC-2 experiment: Final results," *Bull. Russian Acad. Sci., Phys.*, vol. 73, no. 5, pp. 564–567, May 2009, doi: 10.3103/S1062873809050098.

[11] C. C. Finlay *et al.*, "International geomagnetic reference field: The eleventh generation," *Geophys. J. Int.*, vol. 183, no. 3, pp. 1216–1230, Dec. 2010, doi: 10.1111/j.1365-246X.2010.04804.x.

[12] P. Zuccon, "A Monte Carlo simulation of the cosmic rays interactions with the Earth's atmosphere," *Int. J. Mod. Phys. A*, vol. 17, pp. 1625–1634, May 2002.

[13] N. A. Tsyganenko, "Modeling the Earth's magnetospheric magnetic field confined within a realistic magnetopause," *J. Geophys. Res., Space Phys.*, vol. 100, no. A4, pp. 5599–5612, 1995. [Online]. Available: https://agupubs.onlinelibrary.wiley.com/doi/abs/10.1029/94JA03193

[14] N. A. Tsyganenko and M. I. Sitnov, "Modeling the dynamics of the inner magnetosphere during strong geomagnetic storms," *J. Geophys. Res., Space Phys.*, vol. 110, no. A3, 2005, Art. no. A03208. [Online]. Available: https://agupubs.onlinelibrary.wiley.com/doi/abs/10.1029/2004JA010798

[15] M. Bouffard *et al.*, "The HEAO-3 cosmic ray isotope spectrometer," *Astrophys. Space Sci.*, vol. 84, no. 1, pp. 3–33, May 1982.

[16] D. F. Smart and M. A. Shea, "Geomagnetic cutoffs: A review for space dosimetry applications," *Adv. Space Res.*, vol. 14, no. 10, pp. 787–796, Oct. 1994. [Online]. Available: http://www.sciencedirect.com/science/article/pii/0273117794905436

[17] Y. Wei *et al.*, "Performance of the DAMPE BGO calorimeter on the ion beam test," *Nucl. Instrum. Meth. Phys. Res. A, Accel. Spectrom. Detect. Assoc. Equip.*, vol. 922, pp. 177–184, Apr. 2019.